Hindawi
Journal of Chemistry
Volume 2023, Article ID 9753974, 1 page
https://doi.org/10.1155/2023/9753974

Retraction

Retracted: Research on Ethanol Coupling to Prepare C4 Olefins Based on BP Neural Network and Cluster Analysis

Journal of Chemistry

Received 22 August 2023; Accepted 22 August 2023; Published 23 August 2023

This article has been retracted by Hindawi following an investigation undertaken by the publisher [1]. This investigation has uncovered evidence of one or more of the following indicators of systematic manipulation of the publication process:

(1) Discrepancies in scope
(2) Discrepancies in the description of the research reported
(3) Discrepancies between the availability of data and the research described
(4) Inappropriate citations
(5) Incoherent, meaningless and/or irrelevant content included in the article
(6) Peer-review manipulation

The presence of these indicators undermines our confidence in the integrity of the article's content and we cannot, therefore, vouch for its reliability. Please note that this notice is intended solely to alert readers that the content of this article is unreliable. We have not investigated whether authors were aware of or involved in the systematic manipulation of the publication process.

Wiley and Hindawi regrets that the usual quality checks did not identify these issues before publication and have since put additional measures in place to safeguard research integrity.

We wish to credit our own Research Integrity and Research Publishing teams and anonymous and named external researchers and research integrity experts for contributing to this investigation.

The corresponding author, as the representative of all authors, has been given the opportunity to register their agreement or disagreement to this retraction. We have kept a record of any response received.

References

[1] S. Zhang, W. Zhan, H. Hu, Y. Liu, and J. Zhu, "Research on Ethanol Coupling to Prepare C4 Olefins Based on BP Neural Network and Cluster Analysis," *Journal of Chemistry*, vol. 2022, Article ID 5324336, 10 pages, 2022.

Hindawi
Journal of Chemistry
Volume 2022, Article ID 5324336, 10 pages
https://doi.org/10.1155/2022/5324336

Research Article

Research on Ethanol Coupling to Prepare C_4 Olefins Based on BP Neural Network and Cluster Analysis

Sheng-Mei Zhang, Wen-Li Zhan, Han Hu, Yu-Shu Liu, and Jia-Ming Zhu

School of Statistics and Applied Mathematics, Anhui University of Finance and Economics, Bengbu 233030, China

Correspondence should be addressed to Jia-Ming Zhu; zhujm1973@163.com

Received 7 February 2022; Accepted 16 March 2022; Published 26 March 2022

Academic Editor: Haidar Ali

Ethanol, as a clean energy source, is an ideal raw material for the preparation of C_4 olefins, but there are few studies on the preparation of C_4 olefins by the coupling of ethanol. This research is based on the data from Question B of the 2021 Chinese Contemporary Undergraduate Mathematical Contest in Modeling. The researchers firstly perform data interpolation and visualization processing on the original data. Secondly, based on the two-dimensional visualization analysis, we cluster the different catalyst combinations; divide the influencing factors into temperature, Co/SiO_2 and HAP loading ratio, Co loading, and ethanol concentration; and construct a quaternary linear regression equation that affects ethanol conversion rate and C_4 olefin selectivity. Finally, according to the three-dimensional spatial visualization analysis and using the BP neural network model training data, we obtain that under the conditions of using loading method I, catalyst combination type 200 mg 0.5 wt% Co/SiO_2-200 mg HAP-ethanol concentration 0.9 ml/min and temperature 450°C, the yield of C_4 olefins can reach the maximum. This study provides new research ideas and methods for the preparation of C_4 olefins from ethanol.

1. Introduction

On September 11, 2020, General Secretary Xi Jinping mentioned at the symposium of scientists that China still has practical problems such as insufficient development of new energy technologies and excessive oil dependence. In order to implement General Secretary Xi Jinping's strategic thinking on sustainable development and respond to the "14th Five-Year Plan" strategic policy, China has changed the raw material for preparing C_4 olefins from traditionally used petroleum to ethanol. C_4 olefins are widely used in Chinese medicine and industry and are a very important chemical industry production material. In the process of preparing C_4 olefins from ethanol, studying the types of catalyst combinations, temperature changes, and other conditions is of vital significance and value for reducing energy waste and improving reaction effects and productivity.

In recent years, Chinese scholars have conducted various research and explorations on the preparation of C_4 olefins. Peng [1] adopted mixed C_4 alkane dehydrogenation technology to prepare C_4 olefins and used high-temperature solid phase diffusion method and impregnation method to prepare spent FCC catalyst and VO_x/Al_2O_3 catalyst, respectively. It is concluded that the best catalytic performance can be obtained when the VO_x loading in the VO_x/Al_2O_3 catalyst is 12%. Hu [2] used the impregnation method to prepare the supported catalysts and used characterization methods to evaluate certain properties of the prepared catalysts by constructing an evaluation model. He also analyzed the effects of loading and carrier properties on the catalytic process and explored the dehydrogenation effect and catalytic stability of the catalyst under different activity distribution ratios. Li [3] constructed two catalytic systems and analyzed the acid-base performance, surface characteristics, structure, and other aspects of the catalyst using various

technical means which reveals that the configuration of the *tert*-butyl carbocation intermediate determines the anti-*cis* ratio of the product 2-butene in the double-bond isomerization reaction of 1-butene.

At present, Chinese research on the preparation of C_4 olefins is mainly focused on the catalytic dehydrogenation of low-carbon alkanes, while the research on the preparation of C_4 olefins by ethanol coupling mostly stays at the level of experimental research. Based on the above content, this paper further applies mathematical methods to closely link chemical principles and experimental data and studies the reaction of ethanol as a raw material to prepare C_4 olefins from different angles and levels.

2. Basic Assumptions and Index Selection

2.1. Basic Assumptions. In order to facilitate the study of the problem, the following hypotheses are put forward:

(i) The data given conforms to the laws of chemical experiments and is true and effective

(ii) The influence of external factors such as indoor temperature changes and experimental equipment on the experimental data is not considered

(iii) Ignore the influence of factors other than the type of catalyst combination and temperature on the reaction [4]

2.2. Index Selection and Description. The reaction of ethanol coupling to prepare C_4 olefins mainly involves the reactant ethanol, the main product C_4 olefins, the catalyst, and the temperature that has a significant impact on the experiment. After consulting a large amount of data and drawing on previous experience, we finally selected five types of indicators, including catalyst combination, temperature, ethanol conversion rate, C_4 olefin selectivity, and C_4 olefin yield [5], and made the following explanations:

(i) Catalyst combination: including catalyst and reactant. A total of 21 types of catalyst combinations, of which $A_i(i = 1, 2, \cdots, 14)$ catalyst combinations use charging method I and catalyst combinations $B_j(j = 1, 2, \cdots, 7)$ use charging method II. The following are sorted by $A_i = i$ and $B_j = 14 + j$ from the smallest to the largest [6]

(ii) Temperature: refers to the reaction temperature. The temperature data in the text refers to 250°C, 275°C, 300°C, 325°C, 350°C, 400°C, and 450°C

(iii) Ethanol conversion rate: unit: %. Ethanol conversion rate = (ethanol intake − remaining amount of ethanol)/ethanol take × 100% [7]

(iv) C_4 olefin selectivity: unit: %. The greater the selectivity is, the better the experimental results are

(v) C_4 olefin yield: equal to ethanol conversion rate × C_4 olefin selectivity, combined with reactants and products to measure the experimental results [8]

(vi) Loading method: comparing the catalyst combination data numbered A12 and B1, only the charging method is different where the experimental result of A12 is slightly better than that of B1. But the difference is not significant. Therefore, we ignore the influence of this factor and choose the loading method I first [9]

3. Data Preprocessing and Visualization

3.1. Interpolation of Data. There are differences in the data given. The maximum value of the temperature in the experimental data of catalyst combination numbers A1 and A2 is 350°C, while the maximum value of the temperature in the data of the rest of the experimental groups is all higher than 350°C. Among them, the maximum temperature of 18 groups is 400°C, and the maximum value of catalyst combination number A4 is 450°C [10]. For the convenience of follow-up research, spline interpolation [11] is used to fill in missing values, and the repaired interpolation results are shown in Table 1.

In Table 1, the data listed in italic are the repaired missing value, in which the ethanol conversion rate is reserved to 1 decimal place, and the C_4 olefin is selectively reserved to 2 decimal places. The rest are the original data, which serve as a comparison. It can be compared with the data of other temperatures under the same catalyst combination to intuitively judge the accuracy of the interpolation [12].

3.2. Data Visualization

3.2.1. Two-Dimensional Visualization. After interpolation, observe the numerical distribution of ethanol conversion rate and C_4 olefin selectivity for different catalyst combinations at the same temperature in which the temperature is selected as 250°C, 275°C, 300°C, 325°C, 350°C, and 400°C, as shown in Figures 1 and 2, respectively [13].

When the temperature is constant, the greater the value of the ethanol conversion rate and the C_4 olefin selectivity, the better the coupling reaction result, indicating that the catalyst combination effect used in the reaction is better [14]. It can be seen from Figure 1 that the catalysts numbered A1 to A7 have a significant combined effect. From Figure 2, it can be seen that the catalysts numbered A1 and A2 have a significant combined effect. Based on Figures 1 and 2, the reaction results at temperatures of 300°C, 325°C, 350°C, and 400°C are generally better than those at temperatures of 250°C, 275°C, and 300°C [15]. Further, study the reaction results of each catalyst combination at different temperatures. The reaction results are reflected by the ethanol conversion rate and C_4 olefin selectivity. Since there are 21 combinations in total, the representative catalyst combination numbered A7 is selected [16]. And the result is shown in Figure 3.

According to Figure 3, when the temperature is between 250°C and 400°C, both the ethanol conversion rate and the C_4 olefin selectivity are positively correlated with the temperature [17]. As the temperature rises, the values of ethanol conversion rate and C_4 olefin selectivity continue to increase.

Table 1: Spline interpolation to patch missing data.

Catalyst combination type	A1		A2		A6			A7	
Temperature (°C)	350	*400*	350	*400*	300	*325*	350	300	*325*
Ethanol conversion rate (%)	36.8	*51.6*	67.9	*62.7*	25.5	*43.4*	55.8	40	*48.4*
C_4 olefin selectivity (%)	47.21	*62.68*	39.1	*51.46*	7.18	*11.54*	10.65	8.84	*13.90*
Catalyst combination type		A8			A9			A10	
Temperature (°C)	300	*325*	350	300	*325*	350	300	*325*	350
Ethanol conversion rate (%)	13.2	*20.8*	31.7	4.7	*9.3*	13.4	1.7	*3.9*	9.0
C_4 olefin selectivity (%)	13.82	*17.99*	25.89	16.1	*23.39*	31.04	2.17	*3.69*	3.3
Catalyst combination type		A11			A12			A13	
Temperature (°C)	300	*325*	350	300	*325*	350	300	*325*	350
Ethanol conversion rate (%)	1.6	*3.3*	8.2	6.9	*10.9*	19.9	4.1	*8.2*	14.6
C_4 olefin selectivity (%)	1.82	*3.57*	4.35	11.22	*18.93*	22.26	12.74	*17.05*	23.46
Catalyst combination type		A14			B1			B2	
Temperature (°C)	300	*325*	350	300	*325*	350	300	*325*	350
Ethanol conversion rate (%)	10.2	*14.9*	24	6.7	*10.6*	19.3	6.2	*11.6*	16.2
C_4 olefin selectivity (%)	3.61	*6.82*	10.83	12.28	*17.76*	25.97	9.32	*13.58*	22.88

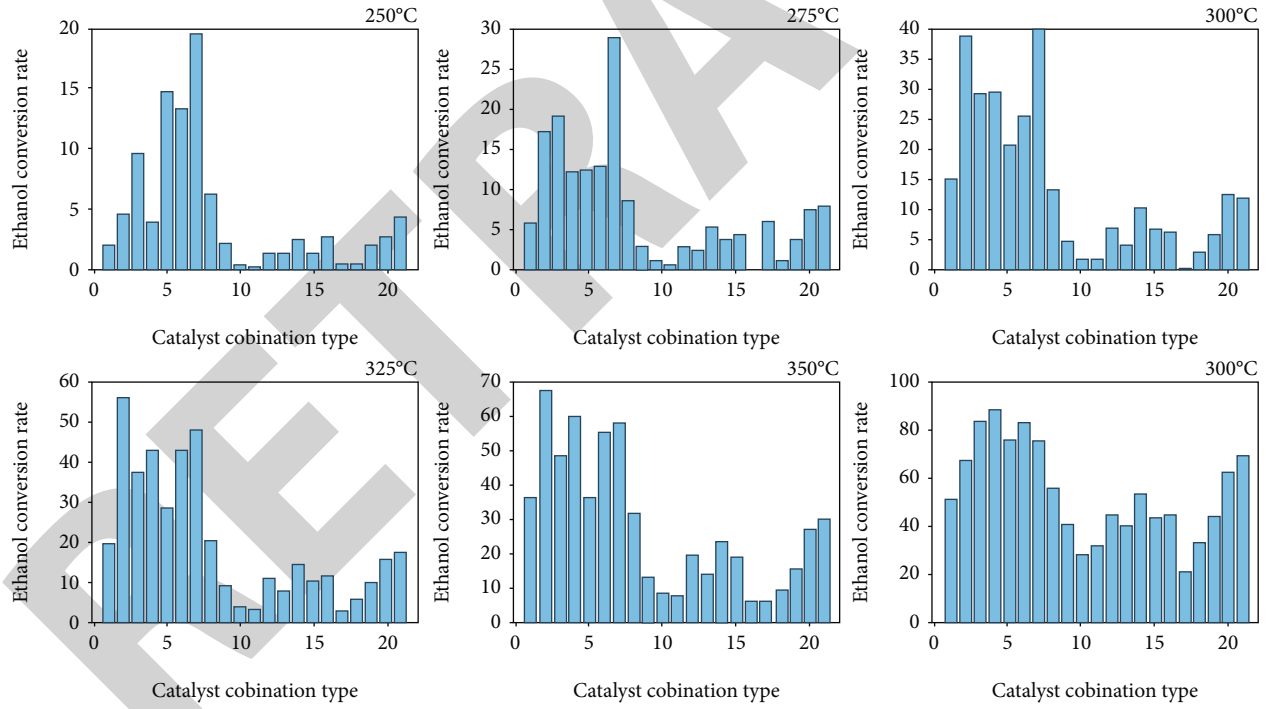

Figure 1: Ethanol conversion rate histogram.

That is, the catalyst group is controlled to remain unchanged, and within a certain temperature range, the reaction result becomes better as the temperature rises [18].

3.2.2. Three-Dimensional Visualization. The spatial distribution of ethanol conversion rate and C_4 olefin selectivity under different catalyst combinations and temperatures [19] are shown in Figures 4 and 5, respectively. It can be seen from the spatial distribution map that there are significant differences in the spatial distribution of ethanol conversion rate and C_4 olefin selectivity [20].

4. Multiple Linear Regression Model Based on Systematic Clustering

According to the two-dimensional visualization processing, when the temperature is between 250°C and 400°C, both the ethanol conversion rate and the C_4 olefin selectivity

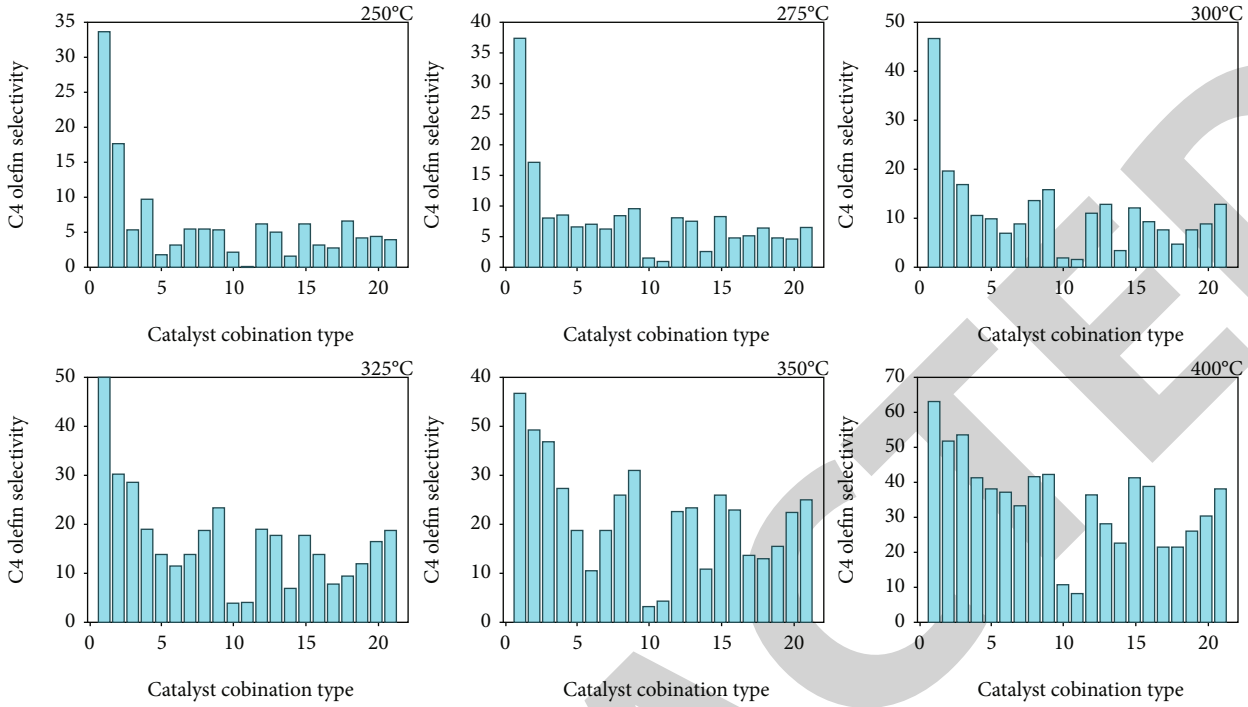

Figure 2: C_4 olefin selectivity histogram.

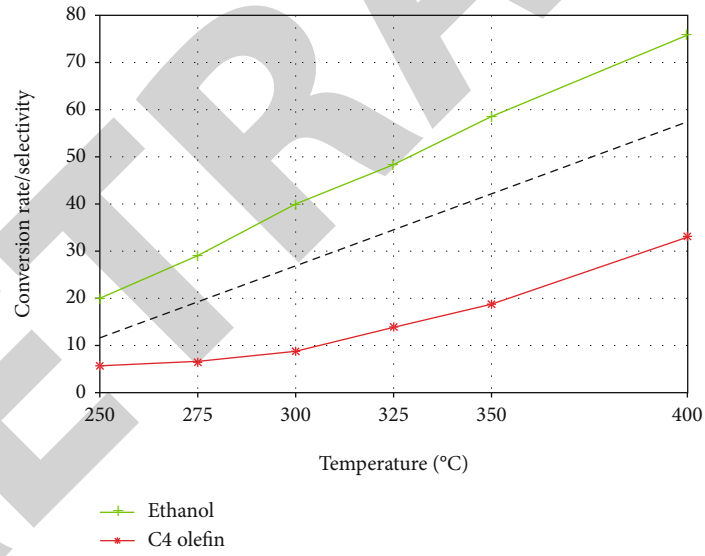

Figure 3: Spatial distribution of ethanol conversion rate.

are positively correlated with the temperature. As the temperature rises, the values of ethanol conversion rate and C_4 olefin selectivity continue to increase. That is, the catalyst group is controlled to remain unchanged, and within a certain temperature range, the reaction result becomes better as the temperature rises [21].

4.1. Model Establishment. Based on the above analysis, a cluster analysis was performed on the catalyst combination, and the reaction results were divided into four categories: "significant," "good," "fair," and "poor." Hierarchical clustering method is used here. According to the distance between the two types of data, the systematic clustering method combines the closest two types of data and repeats the above operations repeatedly until all types of data are clustered into one type [22]. The specific process is as follows:

(i) Divide the catalyst combinations into 21 categories, calculate the distance between each two categories, and find the smallest distance among them

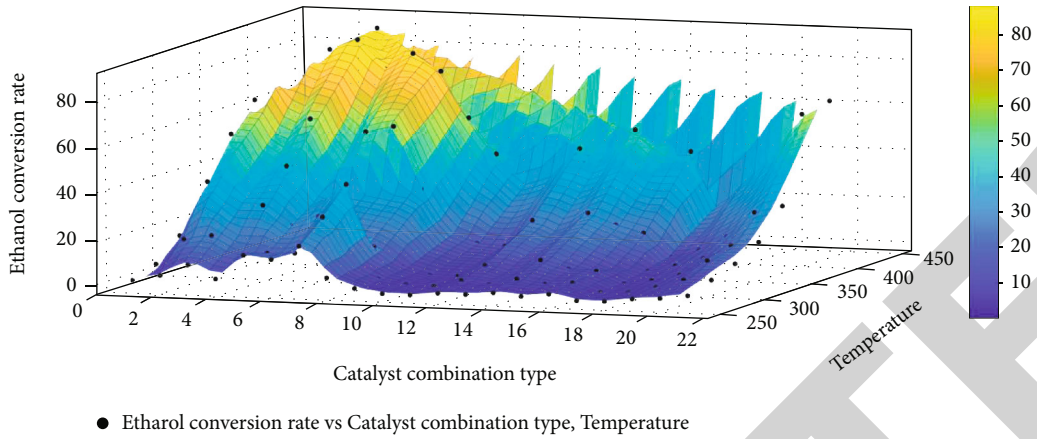

Figure 4: Spatial distribution of ethanol conversion rate.

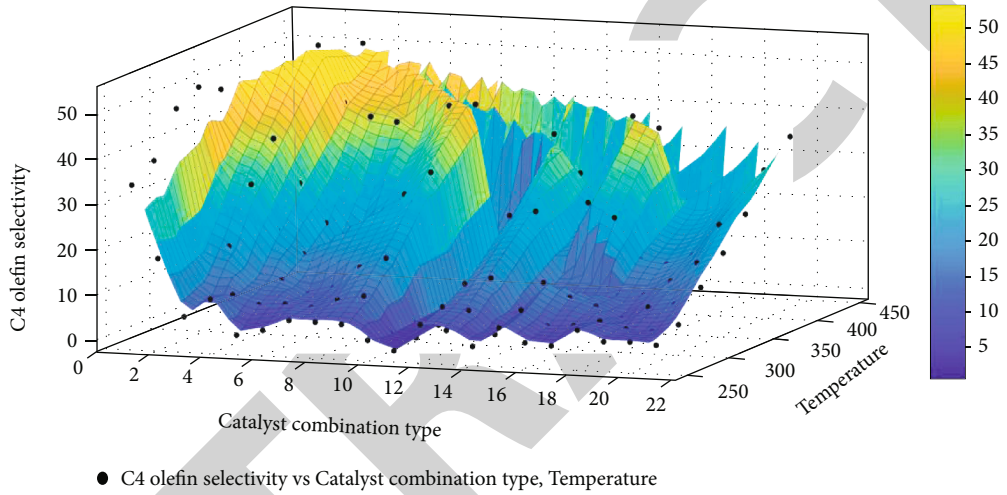

Figure 5: Spatial distribution of C_4 olefin selectivity.

(ii) Put the two catalyst combinations with the smallest distance into a new category, and let this new category and other catalyst combinations that are not in the new category form a new category group

(iii) Calculate the distance between every two categories in the new classification group, and find the minimum distance

(iv) Repeat steps (ii) and (iii), until finally, there is only one category left [23]

The ethanol conversion rate and C_4 olefin selectivity were clustered, respectively, and the reaction results of each catalyst combination were classified according to the obtained clustering pedigree [24]. Using the data under the catalyst group with "significant" reaction results, establish multiple linear regression equations that affect ethanol conversion and C_4 olefin selectivity:

$$y = a_1x_1 + a_2x_2 + \cdots + a_nx_n + b. \quad (1)$$

Take the ethanol conversion rate as an example, where y is the ethanol conversion rate. x_i is the factor that affects the ethanol conversion rate $(i = 1, 2, \cdots, n)$. a_i is the influence coefficient of x_i on y. The larger the coefficient is, the greater the effect $(i = 1, 2, \cdots, n)$ is. b is a constant term, which is jointly determined by y, x_i, and a_i. n is the number of influencing factors [25].

4.2. Model Solution and Analysis. Using SPSS 25 software, the 21 types of catalyst combinations were systematically clustered according to the ethanol conversion rate, and the obtained results are shown in Figure 6.

It can be seen from the pedigree diagram of ethanol conversion rate that

(i) the catalyst combinations that have "significant" effects on the ethanol conversion rate are A2, A4, A5, and A7

(ii) the catalyst combinations that affect "good" are A1, A3, A6, A8, A14, B6, and B7

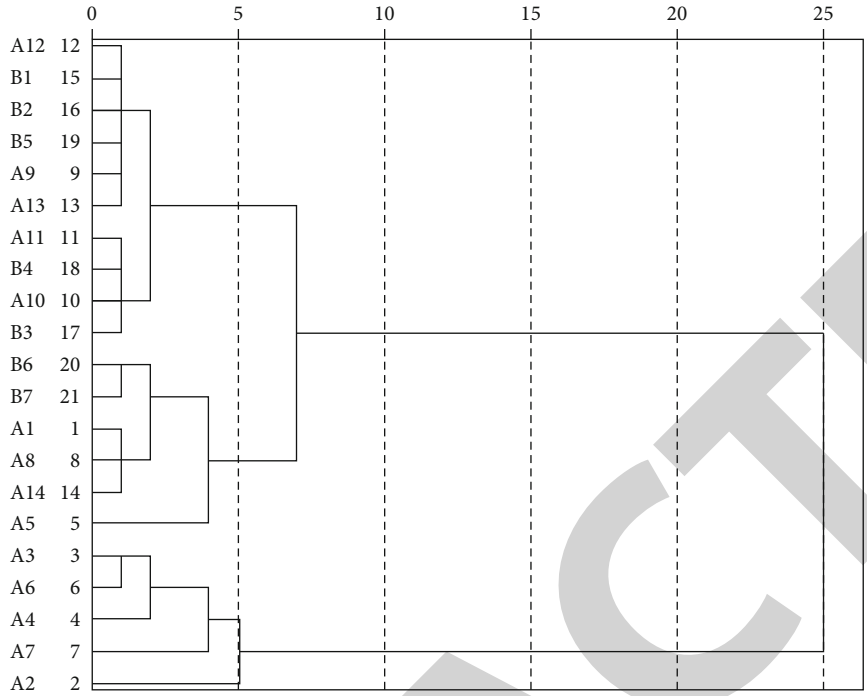

Figure 6: A pedigree of ethanol conversion rate using average linkage (among groups).

(iii) the catalyst combinations that affect "fair" are numbered A9, A12, A13, B1, B2, and B5

(iv) the catalyst combinations that affect "poor" are numbered A10, A11, B3, and B4 [26]

Similarly, using SPSS 25 software to do the same treatment for the C_4 olefin selectivity, the result is shown in Figure 7.

According to the C_4 olefin selectivity clustering pedigree diagram, it can be seen that

(i) the catalyst combinations that "significantly" affect the C_4 olefin selectivity are A1 and A2

(ii) the catalyst combinations that affect "good" are A3 and A9

(iii) the catalyst combinations that affect "fair" are numbered A4, A5, A6, A7, A8, A12, A13, B1, B2, B6, and B7

(iv) the catalyst combinations that affect the "poor" are numbered A10, A11, A14, B3, B4, and B5 [27]

In summary, for the ethanol conversion rate, the catalyst combination numbers A2, A4, A5, and A7 have "significant" effects. For C_4 olefin selectivity, the catalyst combination numbers A1 and A2 have "significant" effects. Analyze the composition of each catalyst combination, and finally, select temperature, Co/SiO_2 and HAP charging ratio (hereinafter referred to as "charge ratio"), Co loading, and ethanol concentration as the main influencing factors and establish a multiple regression equation [28].

Regarding the catalytic efficiency of ethanol, the catalyst combinations numbered A2, A4, A5, and A7 were selected to perform a significant test on the four parameters of temperature, charging ratio, Co loading, and ethanol concentration. Similarly, for the selectivity of C_4 olefins, the catalyst combinations numbered A1 and A2 were selected to test the significance of the four parameters [29]. The test results are shown in Table 2.

It can be seen from Table 2 that for the ethanol conversion rate, the temperature and the charging ratio are very significant, while the Co loading and the dripping rate are more significant. For C_4 olefin selectivity, temperature, charging ratio, and drip rate are very significant, while Co loading is more significant. Temperature, charging ratio, Co loading, and dripping rate can all be used as influencing factors for the study of ethanol conversion rate and C_4 olefin selectivity.

Using Stata software [30], select the catalyst combination data numbered A2, A4, A5, and A7 to perform multiple linear regression on the ethanol conversion rate to obtain the regression equation

$$y_1 = 0.4271x_1 + 0.1020x_2 + 0.6048x_3 - 1.2097x_4 - 118.5026. \quad (2)$$

Similarly, select the catalyst combination data numbered A1 and A2 to perform multiple linear regression on the selectivity of C_4 olefins to obtain the regression equation

$$y_2 = 0.2432x_1 + 0.2259x_2 - 18.132x_3 + 29.8192x_4 - 113.0406, \quad (3)$$

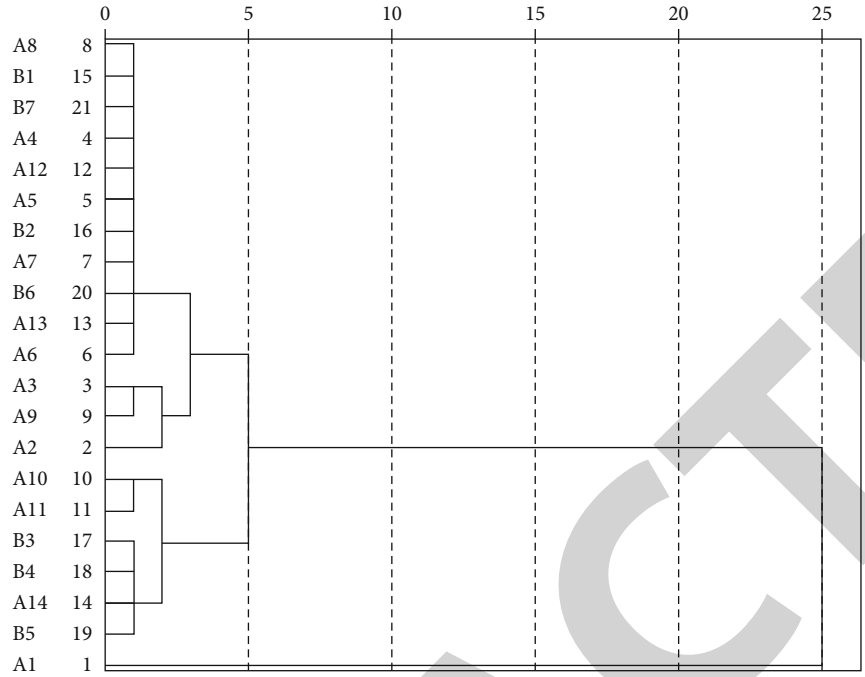

Figure 7: A pedigree of C_4 olefin selectivity using average linkage (among groups).

Table 2: The results of the significance test of each parameter.

Parameter	Temperature	Charge ratio	Co loading	Ethanol concentration
Ethanol conversion rate	$\leq 0.001^{***}$	$\leq 0.001^{***}$	0.008^{**}	0.007^{**}
C_4 olefin selectivity	$\leq 0.001^{***}$	$\leq 0.001^{***}$	0.002^{**}	$\leq 0.001^{***}$

Note: $*$, $**$, and $***$ represent significant, relatively significant, and very significant, respectively.

where x_1 is the temperature, and the temperature range is 250°C-450°C. x_2 is the charging ratio, and the charging ratio range is 10 mg-200 mg/10 mg-200 mg. x_3 is the Co loading, and the Co loading range is 0.5 wt and 5 wt. x_4 is the concentration of ethanol, and the range of ethanol concentration is 0.3 ml/min-2.1 ml/min [31].

5. Exploration on the Optimal Yield of C_4 Olefins Based on BP Neural Network

According to the three-dimensional visualization processing, there are obvious differences in the ethanol conversion rate and the spatial distribution of the C_4 olefin selectivity under the catalyst combination and temperature [32]. Within a given catalyst group and temperature range, we can find a certain catalyst combination and temperature that maximizes the product of the corresponding ethanol conversion rate and C_4 olefin selectivity. Because the yield of C_4 olefins is determined by the conversion of ethanol and the selectivity of C_4 olefins, the catalyst combination and temperature found above are the conditions for maximizing the yield of C_4 olefins [33].

5.1. Research Ideas. The BP neural network is trained according to the error back propagation algorithm and is mainly used in function approximation, pattern recognition, classification, data compression, etc. and is currently one of the most widely used neural network models [34].

The catalyst group in the form of charging ratio, Co loading, ethanol concentration, temperature, ethanol conversion rate, and C_4 olefin selectivity were used as indicators to study the yield of C_4 olefins [35]. For the processed data, select 70% of it as the training set and input it into the neural network model to train the model. Use 15% of the data as a validation set to test the accuracy of the model. Select the remaining 15% of the data as the test set, and constantly adjust the number of hidden layers to achieve the best learning effect [36].

Use the constructed BP neural network model to complete the missing temperature data under the existing catalyst combination. For example, the catalyst combination temperature numbered A1 is only 250°C, 275°C, 300°C, 325°C, and 350°C, and the filling temperature is 251°C, 252°C, …, 349°C. Reuse the existing charging ratio, Co loading, and ethanol concentration to quantify to construct a new catalyst combination. The lowest temperature of the control experiment is 250°C, and the highest temperature is 450°C [37]. The catalyst combination and temperature with the largest product of ethanol conversion rate and C_4 olefin selectivity were selected as the optimal solution of the model [38].

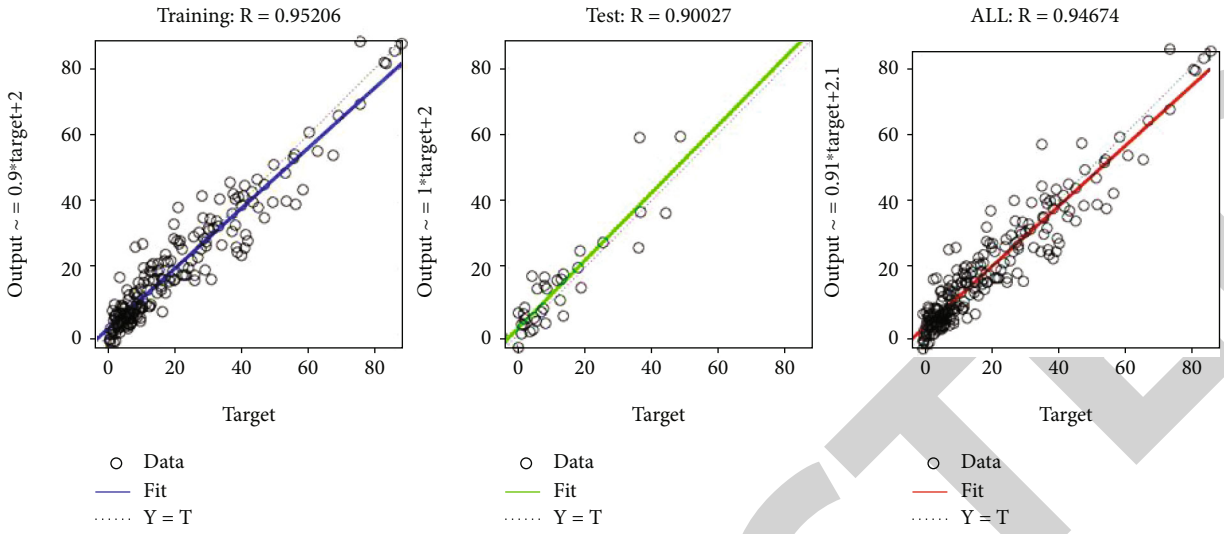

Figure 8: BP neural network fitting effect display.

5.2. Empirical Analysis. After repeated debugging, when the hidden layer of neurons is 15 layers, the fitting effect is better, and the result is shown in Figure 8.

It can be seen from Figure 8 that R^2 of each set is very close to 1 [39]. Under these conditions, the conditions for achieving the maximum yield of C_4 olefins are to use the loading method I, the catalyst type is 200 mg 0.5 wt% Co/SiO_2-200 mg HAP-ethanol concentration 0.9 ml/min, the temperature is 450°C, and the C_4 olefin yield is 48% [40].

6. Conclusion

Based on software such as SPSS 25 and Stata, this article selects Annex 1 of the 2021 Chinese Contemporary Undergraduate Mathematical Contest in Modeling as the research data [41]. According to the reaction process of ethanol coupling to produce C_4 olefins, the research content is divided into two parts. One is to study the factors affecting the ethanol conversion rate and the selectivity of C_4 olefins, and the other is to study the experimental conditions for obtaining the maximum yield of C_4 olefins [42].

For the former, we study the ethanol conversion rate and C_4 olefin selectivity, respectively, and use the ethanol conversion rate as an example to illustrate. First, through cluster analysis, class, and process all catalyst combinations, select the groups with "significant" impact on the ethanol conversion rate [43]. Then, on the basis of the experimental data of the "significant" catalyst groups, select temperature, charging ratio, Co loading, and ethanol concentration as the main influencing factors; carry out the significance test of these four parameters; and screen for significant factors. Finally, with the ethanol conversion rate as the dependent variable and the significant factor as the independent variable, we establish a multiple linear regression model based on cluster analysis [44].

For the latter, we fill in the missing temperature data, add new catalyst groups, and build an optimal model for the yield of C_4 olefins based on BP neural network. Then, we select the group with the largest product of ethanol conversion rate and C_4 olefin as the condition with the largest C_4 olefin yield [45].

Data Availability

The data in this paper come from Question B of the 2021 Chinese Contemporary Undergraduate Mathematical Contest in Modeling.

Conflicts of Interest

The authors declare that there are no conflicts of interest regarding the publication of this paper.

Authors' Contributions

Sheng-Mei Zhang was responsible for the methodology, conceptualization, supervision, and leadership. Wen-Li Zhan was responsible for the conceptualization, visualization, software, validation; and writing the manuscript. Han Hu was responsible for the software, method design, validation, and data analysis. Yu-Shu Liu was responsible for the data collation, visualization, verification, and investigation. Jia-Ming Zhu was responsible for the verification, supervision, writing, reviewing, and editing.

Acknowledgments

This study was funded by the National Social Science Fund Project of China (21CTJ024) and the Teaching and Research Fund Project of the Anhui University of Finance and Economics (acxkjs2021005 and acyljc2021002).

References

[1] Y. F. Peng, *Dehydrogenation of C4 paraffins to C4 olefins, [M.S. thesis]*, China University of Petroleum (East China), Qinhai, China, 2011.

[2] C. Hu, *Calytic dehydrogenation of C4 paraffins to C4 olefins, [M.S. thesis]*, China University of Petroleum (East China), Qinhai, China, 2012.

[3] Y. Li, *Catalyst preparation and reaction mechanism for green catalytic synthesis of C4 olefins, [Ph.D. thesis]*, University of Chinese Academy of Sciences, Beijing, China, 2016.

[4] T. Rajasekhar, U. Haldar, P. De, J. Emert, and R. Faust, "Cationic copolymerization and multicomponent polymerization of isobutylene with C4 olefins," *Macromolecules*, vol. 50, no. 21, pp. 8325–8333, 2017.

[5] P. Cao, L. Zheng, W. Sun, and L. Zhao, "Multiscale modeling of isobutane alkylation with mixed C4 olefins using sulfuric acid as catalyst," *Industrial & Engineering Chemistry Research*, vol. 58, no. 16, pp. 6340–6349, 2019.

[6] N. H. Jabarulla, "Production of olefins from syngas over Al_2O_3 supported Ni and Cu nano-catalysts," *Petroleum Science and Technology*, vol. 37, no. 4, pp. 382–385, 2019.

[7] L. Yang, Y. J. Wu, X. J. Wu, and W. Cai, "High-throughput screening of real metal-organic frameworks for adsorption separation of C4 olefins," *Acta Chimica Sinica*, vol. 79, no. 4, pp. 520–529, 2021.

[8] A. H. Assen, T. Virdis, W. De Moor et al., "Kinetic separation of C_4 olefins using Y-fum-fcu-MOF with ultra-fine-tuned aperture size," *Chemical Engineering Journal*, vol. 413, article 127388, 2020.

[9] J. Cui, Z. Zhang, J. Hu et al., "Geometry control of adsorption sites in sulfonate-pillared hybrid ultramicroporous materials for efficient C4 olefin separations," *Chemical Engineering Journal*, vol. 425, article 130580, 2021.

[10] V. M. Phung and V. L. Tang, "Bivariate Hermite interpolation on the exponential curve," *Periodica Mathematica Hungarica*, vol. 78, no. 2, pp. 166–177, 2019.

[11] X. Tang, L. Wang, and W. Liu, "A comprehensive interpolation for medical slices based on combination of linear and matching interpolation," *Chinese Journal of Electronics*, vol. 20, no. 1, pp. 82–84, 2011.

[12] M. Zhang and X. Z. Liang, "On a Hermite interpolation on the sphere," *Applied Numerical Mathematics*, vol. 61, no. 5, pp. 666–674, 2011.

[13] Y. Fang, H. Ying, X. B. Lai, X. Xu, and X. Ruan, "Visualization analysis of heart diseases using two-dimensional electrocardiogram sequences," *International Journal of Adaptive Control and Signal Processing*, vol. 33, no. 8, pp. 1281–1291, 2019.

[14] A. Jaberi and M. Tadjfar, "Visualization of two-dimensional liquid sheets issued into subsonic gaseous crossflow," *Journal of Visualization*, vol. 23, no. 4, pp. 605–624, 2020.

[15] X. Y. Cui, W. Y. Shi, and C. Lu, "Large-scale visualization of the dispersion of liquid-exfoliated two-dimensional nanosheets," *Chemical Communications*, vol. 57, no. 35, pp. 4303–4306, 2021.

[16] M. Kallio, M. Kivilompolo, S. Varjo, M. Jussila, and T. Hyötyläinen, "Data analysis programs for comprehensive two-dimensional chromatography," *Journal of Chromatography A*, vol. 1216, no. 14, pp. 2923–2927, 2009.

[17] M. Fayed, H. A. Abderrahmane, and H. D. Ng, "Flow visualization and numerical simulation of a two-dimensional fluid flow over a foil," *Journal of Visualization*, vol. 20, no. 4, pp. 687–693, 2017.

[18] H. F. Xu, D. F. Wang, W. D. Li, L. Ma, X. Guo, and Y. Ni, "Three-dimensional visualization technology in coronary-pulmonary artery fistula," *Journal of Cardiac Surgery*, vol. 34, no. 10, pp. 1094–1096, 2019.

[19] V. P. Demkin, Y. S. Pekker, and K. S. Brazovskii, "Radiation diagnostics: application of supercomputer technologies for three-dimensional visualization of biological objects," *Russian Physics Journal*, vol. 55, no. 7, pp. 858-859, 2012.

[20] M. Fischer, G. Strauß, S. Gahr et al., "Dreidimensionale bildprozessierung in der HNO-onkologie zur präoperativen planung und evaluierung," *Laryngo-Rhino-Otologie*, vol. 88, no. 4, pp. 229–233, 2009.

[21] N. Serban and H. J. Jiang, "Multilevel functional clustering analysis," *Biometrics*, vol. 68, no. 3, pp. 805–814, 2012.

[22] P. Y. Mok, H. Q. Huang, Y. L. Kwok, and J. S. Au, "A robust adaptive clustering analysis method for automatic identification of clusters," *Pattern Recognition*, vol. 45, no. 8, pp. 3017–3033, 2012.

[23] A. Obadic and L. Tijanic, "Multivariate analysis of the Croatian clusters," *Economic Research-Ekonomska Istrazivanja*, vol. 27, no. 1, pp. 120–133, 2014.

[24] S. F. Altschul and A. F. Neuwald, "Initial cluster analysis," *Journal of Computational Biology*, vol. 25, no. 2, pp. 121–129, 2018.

[25] L. Y. Wei and C. H. Cheng, "An entropy clustering analysis based on genetic algorithm," *Journal of Intelligent & Fuzzy Systems*, vol. 19, no. 4-5, pp. 235–241, 2008.

[26] R. Ramon-Gonen and R. Gelbard, "Cluster evolution analysis: identification and detection of similar clusters and migration patterns," *Expert Systems with Applications*, vol. 83, pp. 363–378, 2017.

[27] J. R. Kettenring, "A patent analysis of cluster analysis," *Applied Stochastic Models in Business and Industry*, vol. 25, no. 4, pp. 460–467, 2009.

[28] D. Crowther, S. Kim, J. Lee, J. Lim, and S. Loewen, "Methodological synthesis of cluster analysis in second language research," *Language Learning*, vol. 71, no. 1, pp. 99–130, 2021.

[29] A. Cernian, D. Carstoiu, A. Olteanu, and V. Sgarciu, "An integrated cluster analysis and validity test platform for the compression based clustering approach," *Studies in Informatics and Control*, vol. 24, no. 2, pp. 151–158, 2015.

[30] S. F. Ding, H. J. Jia, J. R. Chen, and F. Jin, "Granular neural networks," *Artificial Intelligence Review*, vol. 41, no. 3, pp. 373–384, 2014.

[31] H. M. Liao, S. F. Ding, M. M. Wang, and G. Ma, "An overview on rough neural networks," *Neural Computing & Applications*, vol. 27, no. 7, pp. 1805–1816, 2016.

[32] L. Zhang, F. L. Wang, T. Sun, and B. Xu, "A constrained optimization method based on BP neural network," *Neural Computing & Applications*, vol. 29, no. 2, pp. 413–421, 2018.

[33] X. H. Chen, M. J. Zhang, K. Ruan, C. Gong, Y. Zhang, and S. X. Yang, "A ranging model based on BP neural network," *Intelligent Automation and Soft Computing*, vol. 22, no. 2, pp. 325–329, 2016.

[34] A. Jaberi and M. Tadjfar, "Wavelet-content-adaptive BP neural network-based deinterlacing algorithm," *Soft Computing*, vol. 22, no. 5, pp. 1595–1601, 2018.

[35] S. Dong, D. D. Zhou, W. G. Zhou, W. Ding, and J. Gong, "Research on network traffic identification based on improved BP neural network," *Applied Mathematics & Information Sciences*, vol. 7, no. 1, pp. 389–398, 2013.

[36] K. Cui and X. Jing, "Research on prediction model of geotechnical parameters based on BP neural network," *Neural Computing & Applications*, vol. 31, no. 12, pp. 8205–8215, 2019.

[37] X. Wang, Y. J. Wu, R. J. Wang, Y. Y. Wei, and Y. M. Gui, "Gray BP neural network based prediction of rice protein interaction network," *Cluster Computing*, vol. 22, no. S2, pp. 4165–4171, 2019.

[38] Q. Liu, S. X. Liu, G. Y. Wang, and S. Xia, "Social relationship prediction across networks using tri-training BP neural networks," *Neurocomputing*, vol. 401, pp. 377–391, 2020.

[39] X. G. Li and J. F. Wang, "Traffic detection of transmission of botnet threat using BP neural network," *Neural Network World*, vol. 28, no. 6, pp. 511–521, 2018.

[40] J.-M. Zhu, Y. Chen, and S. Zhang, "Analysis of the impact of climate change on national vulnerability based on fuzzy comprehensive evaluation," *Discrete Dynamics in Nature and Society*, vol. 2020, Article ID 3527540, 10 pages, 2020.

[41] J. B. Liu, C. Wang, S. Wang, and B. Wei, "Zagreb indices and multiplicative Zagreb indices of Eulerian graphs," *Bulletin of the Malaysian Mathematical Sciences Society*, vol. 42, no. 1, pp. 67–78, 2019.

[42] J.-B. Liu, J. Zhao, H. L. He, and Z. Shao, "Valency-based topological descriptors and structural property of the generalized Sierpiński networks," *Journal of Statistical Physics*, vol. 177, no. 6, pp. 1131–1147, 2019.

[43] Q. He, P. Xia, B. Li, and J. B. Liu, "Evaluating investors' recognition abilities for risk and profit in online loan markets using nonlinear models and financial big data," *Journal of Function Spaces*, vol. 2021, Article ID 5178970, 15 pages, 2021.

[44] X. W. Cai, Y. Q. Bao, M. F. Hu, J. B. Liu, and J. M. Zhu, "Simulation and prediction of fungal community evolution based on RBF neural network," *Computational and Mathematical Methods in Medicine*, vol. 2021, Article ID 7918192, 13 pages, 2021.

[45] J. M. Zhu, N. Dehgardi, and X. Li, "The third leap Zagreb index for trees," *Journal of Chemistry*, vol. 2019, Article ID 9296401, 6 pages, 2019.